Naval Research Laboratory

Washington, DC 20375-5000

NRL Memorandum Report 6180

Nonlinear Theory of Phase Locking Gyrotron Oscillators Driven by an External Signal

A. W. FLIFLET AND W. M. MANHEIMER

Plasma Physics Division

July 15, 1988

SECURITY CLASSIFICATION OF THIS PAGE

REPORT DOCUMENTATION PAGE

Form Approved OMB No 0704-0188

1a REPORT SECURITY CLASSIFICATION: UNCLASSIFIED	1b RESTRICTIVE MARKINGS
2a SECURITY CLASSIFICATION AUTHORITY	3 DISTRIBUTION/AVAILABILITY OF REPORT: Approved for public release; distribution unlimited.
2b DECLASSIFICATION/DOWNGRADING SCHEDULE	
4 PERFORMING ORGANIZATION REPORT NUMBER(S): NRL Memorandum Report 6180	5 MONITORING ORGANIZATION REPORT NUMBER(S)
6a NAME OF PERFORMING ORGANIZATION: Naval Research Laboratory; 6b OFFICE SYMBOL (If applicable): Code 4740	7a NAME OF MONITORING ORGANIZATION
6c ADDRESS (City, State, and ZIP Code): Washington, DC 20375-5000	7b ADDRESS (City, State, and ZIP Code)
8a NAME OF FUNDING/SPONSORING ORGANIZATION: SDIO/Innovative Science and Technology; 8b OFFICE SYMBOL (If applicable)	9 PROCUREMENT INSTRUMENT IDENTIFICATION NUMBER
8c ADDRESS (City, State, and ZIP Code): Washington, DC 20301	10 SOURCE OF FUNDING NUMBERS: PROGRAM ELEMENT NO: 66000A; PROJECT NO: ; TASK NO: 0; WORK UNIT ACCESSION NO: DN156-218

11 TITLE (Include Security Classification)

Nonlinear Theory of Phase Locking Gyrotron Oscillators Driven by an External Signal

12 PERSONAL AUTHOR(S)

Fliflet, A.W. and Manheimer, W.M.

13a TYPE OF REPORT	13b TIME COVERED	14 DATE OF REPORT (Year, Month, Day)	15 PAGE COUNT
Interim	FROM 1/87 TO 12/87	1988 July 15	54

16 SUPPLEMENTARY NOTATION

17 COSATI CODES			18 SUBJECT TERMS (Continue on reverse if necessary and identify by block number)
FIELD	GROUP	SUB-GROUP	Phase-locked operation; Direct injection; Prebunching cavity; Perturbation; AC current density; Phase-locking bandwidth

19 ABSTRACT (Continue on reverse if necessary and identify by block number)

A time-dependent slow-time-scale theory is developed for gyrotron oscillators driven by an external signal. The signal is introduced either directly into the cavity output or via a beam prebunching cavity. The theory is applied to a high voltage gyrotron configuration and the numerical, nonlinear calculations are compared with simple analytical estimates of the frequency bandwidth for phase-locked operation. For the case of direct injection, the non-linear slow-time-scale calculations are in good agreement with Adler's relation. Two approaches are investigated for the case of phase-locking with a prebunching cavity. In the first the induced ac current density due to the prebunching cavity is treated as a small perturbation on the ac current density in the oscillator. In

(Continues)

20 DISTRIBUTION/AVAILABILITY OF ABSTRACT	21 ABSTRACT SECURITY CLASSIFICATION
☒ UNCLASSIFIED/UNLIMITED ☐ SAME AS RPT ☐ DTIC USERS	UNCLASSIFIED
22a NAME OF RESPONSIBLE INDIVIDUAL: Arne W. Fliflet	22b TELEPHONE (Include Area Code): (202) 767-2469; 22c OFFICE SYMBOL: Code 4740

DD Form 1473, JUN 86 Previous editions are obsolete SECURITY CLASSIFICATION OF THIS PAGE

19. ABSTRACT (Continued)

this approach the equations for the time-dependent wave amplitude and phase are similar in structure to the equations for gyrotrons driven by direct injection and lead to a simple analytical estimate of the locking bandwidth. The accuracy of the perturbation approach is investigated by comparing it with the results of an alternate approach used in the analysis of gyro-klystrons. The maximum phase-locking bandwidth obtainable with the prebunching cavity approach is discussed.

Accession For	
NTIS GRA&I	☑
DTIC TAB	☐
Unannounced	☐
Justification	
By	
Distribution/	
Availability Codes	
Dist	Avail and/or Special
A-1	

CONTENTS

NONLINEAR THEORY OF PHASE LOCKING GYROTRON OSCILLATORS DRIVEN BY AN EXTERNAL SIGNAL

I. INTRODUCTION

There is currently considerable interest in the development of high power phase-locked gyrotron oscillators. These devices have the potential to combine the high efficiency and power associated with oscillators with the coherence and phase control properties associated with amplifiers. Although previous theoretical work on steady-state gyrotron operation[1-8] has been successfully applied to the development of cw devices for heating of tokamak plasmas, the investigation of the phase locking of gyrotron oscillators driven by external signals has received much less attention. A consideration of the properties of driven oscillators necessarily involves the study of non-stationary operation. Time dependent effects can be studied using a particle-in-cell simulation code of the type developed by Lin and co-workers [9]. In this work an alternative nonlinear, slow-time-scale approach is used to study time-dependent effects in driven oscillators. Under certain approximations analytical estimates of such quantities as the locking bandwidth are obtained. For example, Adler's relation [10] is recovered for the case of phase locking by direct injection of radiation at the cavity output.

The time-dependent theory of gyrotrons has been considered by Nusinovich and co-workers [11,12], mainly in the context of multimode operation and mode stability. A time dependent multimode theory of quasi-optical gyrotrons has been developed by Bondeson et al.[13]. Early work on mode selection and phase-

Manuscript approved February 5, 1988.

locking of vacuum tube oscillators was carried out by Van der Pol [14] and Adler [10]. An analytical theory of the conditions for phase-locking gyrotrons has been presented by Manheimer [15,16]. The present work extends the theoretical approach developed by Manheimer to the nonlinear regime and incorporates slow-time-scale (STS) gyrotron dynamics.

The time dependent theory of driven gyrotron oscillators derived in this work is based on slow-time-scale equations for the electron motion similar to those used in steady-state models [7,17,18]. Slow-time-scale equations for the cavity rf field amplitude are obtained by expressing the time-dependent behavior relative to a reference frequency ω_o which is close to the operating frequency ω. The fact that the electron transit time through the cavity is short compared to the radiation field risetime is also exploited. The external signal is introduced either directly into the cavity output or via a beam prebunching cavity. Two approaches are investigated for the case of phase-locking with a prebunching cavity. In the first the induced ac current density due to the prebunching cavity is treated as a small perturbation on the ac current density in the oscillator. In this approach, which follows the work of Manheimer [16], the equations for the time-dependent wave amplitude and phase are similar in structure to the equations for gyrotrons driven by direct injection and lead to a simple analytical estimate of the locking bandwidth. The accuracy of the perturbation approach is investigated by comparing it with the results of the second approach in which the beam prebunching is introduced in the

initial conditions for integrating the equations-of-motion. This approach is well-known in the analysis of gyro-klystons [19]. The theory is applied to a high voltage gyrotron configuration similar to the NRL high voltage gyrotron experiment [17].

The next section of this paper describes the theoretical approach. The following section contains the results of calculations. Section IV presents conclusions drawn from this research and discusses the maximum bandwidth obtainable using a prebunching cavity. The last section contains our acknowledgements.

II. THEORY

Consider a gyrotron with a cylindrical resonator and a thin annular beam. The electrons follow helical trajectories in the applied axial magnetic field about guiding centers located at a radius R_o from the symmetry axis. The electron beam interacts with a TE resonator mode which is assumed to be near cutoff. It is convenient to look at time dependent effects which remain after a reference frequency ω_o has been factored out. These effects are characterized by time scales which are much longer than the wave period and are incorporated in a time dependent mode profile function f(z,t). Using complex notation, the transverse electric field is expressed in the form:

$$\mathbf{E}_t = f(z,t)\mathbf{e}_n(r,\theta;z)\exp(-i\omega_o t) \qquad (1)$$

where $\mathbf{e}_n = \mathbf{z}\times\nabla_t\psi$ is the waveguide transverse-mode vector function and ψ is the corresponding scalar mode function which satisfies a Helmholtz equation with respect to the transverse coordinates [18]. The transverse electric field satisfies the wave equation:

$$\nabla^2\mathbf{E}_t - \frac{1}{c^2}\frac{\partial^2\mathbf{E}_t}{\partial t^2} = \mu_o\frac{\partial\mathbf{J}_t}{\partial t} \qquad (2)$$

where $\mathbf{J}_t$ is the transverse ac current density, c is the speed of light and μ_o is the permeability of free space. MKS units are used throughout except as noted.

There are two methods of phase-locking gyrotron oscillators: direct injection of a locking signal or by means of a modulated

electron beam produced by a prebunching cavity. In the case of direct injection of radiation the wave amplitude function at the cavity output can be expressed in the form:

$$f(z,t) = A(t)e^{i[k_z z-\psi(t)]} + \beta e^{-ik_{z_o} z} \qquad (3)$$

where the first term on the right hand side of Eq.(3) represents the time-dependent oscillator output (an outgoing wave with amplitude A and wavenumber k_z; ψ is a slowly varying phase) and the second term represents a constant amplitude incoming wave with frequency ω_o due to the external signal. In the case of beam premodulation via a bunching cavity, the ac current density can be viewed as having two parts:

$$J_t = J + \delta J \qquad (4)$$

where J is generated by the electric field in the oscillator cavity and δJ is the current density generated in the prebunching cavity. It is convenient to express the rf current density in the approximate form [7]:

$$J_t = (J_\omega + \delta J_\omega)\exp(-i\omega_o t) \qquad (5)$$

where

$$J_\omega = \int_0^{2\pi} d(\omega_o t)\ J\ e^{i\omega_o t} \qquad (6)$$

and similarly for δJ_ω. Substituting Eqs.(1) and (5) into Eq.(2), noting that $\partial f/\partial t << \omega_o f$, multiplying by e_n^*, and integrating over the resonator cross section one obtains:

$$\left[\frac{\partial^2}{\partial z^2} + \frac{\omega_o^2-\omega_{co}^2}{c^2} + 2i\frac{\omega_o}{c^2}\frac{\partial}{\partial t}\right] f(z,t) = -i\mu_o\omega_o \int da\ e_n^*\cdot(J_\omega+\delta J_\omega) \tag{7}$$

where ω_{co} is the cut-off frequency of the resonant mode in the cavity.

To obtain slow-time-scale equations for a gyrotron oscillator driven by an external signal, multiply Eq.(7) by f^* and multiply the complex conjugate of Eq.(7) by f. Then first add and then subtract the resulting equations, and integrate the sum or difference over the axial extent of the cavity. The sum leads to:

$$\int_0^L dz\left[f^*\frac{\partial^2 f}{\partial z^2} + f\frac{\partial^2 f^*}{\partial z^2} + 2\frac{\omega_o^2-\omega_{co}^2}{c^2}ff^* + 2i\frac{\omega_o}{c^2}\left(f^*\frac{\partial f}{\partial t} - f\frac{\delta f^*}{\delta t}\right)\right] =$$

$$-i\mu_o\omega_o\int_V dadz\left[f^*e^*\cdot(J_\omega+\delta J_\omega) - fe\cdot(J_\omega^*+\delta J_\omega^*)\right] \tag{8a}$$

where V denotes integration over the cavity volume. The difference leads to:

$$\int_0^L dz\left[f^*\frac{\partial^2 f}{\partial z^2} - f\frac{\partial^2 f^*}{\partial z^2} + 2i\frac{\omega_o}{c^2}\frac{\partial|f|^2}{\partial t}\right] =$$

$$-i\mu_o\omega_o\int_V dadz\left[f^*e^*\cdot(J_\omega+\delta J_\omega) + fe\cdot(J_\omega^*+\delta J_\omega^*)\right] \qquad (8b)$$

As will be shown, Eq.(8a) leads to an equation for the wave phase and Eq.(8b) leads to an equation for the wave amplitude. Integrating the first two terms on the right hand side of these equations by parts leads to:

$$\frac{\partial|f|^2}{\partial z}\bigg|_0^L + \int_0^L dz\left[-2\left|\frac{\partial f}{\partial z}\right|^2 + 2\frac{(\omega_o^2-\omega_{co}^2)}{c^2}|f|^2 + 2i\frac{\omega_o}{c^2}(f^*\frac{\partial f}{\partial t} - f\frac{\partial f^*}{\partial t})\right] =$$

$$-i\mu_o\omega_o\int_V dadz\left[f^*e^*\cdot(J_\omega+\delta J_\omega) - fe\cdot(J_\omega^*+\delta J_\omega^*)\right] \qquad (9a)$$

and:

$$\left[f^*\frac{\partial f}{\partial z} - f\frac{\partial f^*}{\partial z}\right]\bigg|_0^L + 2i\frac{\omega_o}{c^2}\int_0^L dz\,\frac{\partial|f|^2}{\partial t} =$$

$$-i\mu_o\omega_o\int_V dadz\left[f^*e^*\cdot(J_\omega+\delta J_\omega) + fe\cdot(J_\omega^*+\delta J_\omega^*)\right] \qquad (9b)$$

respectively. The first term on the left hand side of Eq.(9a) is a boundary term which vanishes for a free running oscillator

because $f \to 0$ at the cavity input ($z=0$) and $|f|$=constant at the cavity output ($z=L$) when there is only an outgoing wave. The boundary term does not vanish when there is an external signal incident at the cavity output, thus this term corresponds to phase-locking by direct injection of radiation. The boundary term in Eq.(9b) corresponds to the net power flow from the cavity.

In the case of direct injection of radiation (the case of phase-locking via beam prebunching is treated below), the boundary term in Eq.(9a) can be written in the form:

$$\left.\frac{\partial |f|^2}{\partial z}\right|_0^L = -4k_{z_o}A(t)\beta\sin[2k_{z_o}L-\psi(t)] \qquad (10a)$$

and the boundary term in Eq.(9b) can be written in the form:

$$\left[f^*\frac{\partial f}{\partial z} - f\frac{\partial f^*}{\partial z}\right]\Bigg|_0^L = 2ik_{z_o}(A(t)^2-\beta^2) \qquad (10b)$$

where Eq.(3) has been used and the difference between k_z and k_{z_o} has been neglected. Following common practice, the wave amplitude function inside the cavity is written in the separable form:

$$f(z,t) = a(t)e^{-i\psi(t)}h(z) \qquad (11)$$

where h(z) is the axial profile function. In what follows, h(z) will be assumed to have a gaussian form: $h(z)=\exp[-(\kappa_z z)^2]$, centered at the cavity midpoint, where κ_z is the effective axial wavenumber inside the cavity. Using Eq.(11) in Eq.(9a) and (9b) and substituting Eq.(10a) or (10b) for the boundary terms leads to:

$$-4k_{z_o}A(t)\beta\sin[2k_{z_o}L-\psi(t)] + 2N\left[\frac{\omega_o^2-\omega_{r_o}^2}{c^2}a(t)^2 + 2\frac{\omega_o}{c^2}a(t)^2\dot{\psi}\right] =$$

$$-i\mu_o\omega_o a(t)\int_V dadzh(z)\left[e^*\cdot J_\omega e^{i\psi} - e\cdot J_\omega^* e^{-i\psi}\right] \qquad (12a)$$

from Eq.(9a); and

$$2k_{z_o}[A(t)^2-\beta^2] + 4\frac{\omega_o}{c^2}a(t)\dot{a}(t)N =$$

$$-\mu_o\omega_o a(t)\int_V dadzh(z)\left[e^*\cdot J_\omega e^{i\psi} + e\cdot J_\omega^* e^{-i\psi}\right] \qquad (12b)$$

from Eq.(9b);

where:

$$N = \int_0^L dz|h(z)|^2 \simeq \sqrt{\frac{\pi}{2}}\frac{L}{2} \qquad (13)$$

for a gaussian profile, and ω_{r_o} is the cold cavity eigenfrequency of the interacting mode.

To calculate the ac current density, the interaction with the electron beam is treated in the single particle approximation. A considerable simplification of the general time dependent problem results if one uses the fact that the characteristic rise time of fields in the resonator is much longer than the electron transit time in the cavity. In this case one can use a quasi-steady-state approximation in which the electron trajectories are calculated for rf fields with fixed amplitude, $f(\tau_o)$, and linearized phase, $\psi=\psi'(\tau_o)(\tau-\tau_o)$. The slow-time-scale nonlinear electron equations of motion for an electron in a thin annular beam interacting at a particular harmonic with a single circularly polarized TE mode are readily deduced from previous steady-state analyses [7,18] and are given by:

$$\frac{du_t}{d\bar{z}} = -\frac{\gamma}{u_z} f J_s'(\bar{k}_t \bar{r}_L) \, Re\left[\left(h + i\frac{u_z}{\gamma\bar{\omega}_o}\frac{dh}{d\bar{z}}\right)e^{-i[\Lambda+\psi]}\right] \tag{14a}$$

$$\frac{d\Lambda}{d\bar{z}} = -\frac{s\gamma}{u_z u_t} f \frac{sJ_s(\bar{k}_t \bar{r}_L)}{\bar{k}_n \bar{r}_L} Re\left[\left(h + i\frac{u_z}{\gamma\bar{\omega}_o}\frac{dh}{d\bar{z}} - \frac{\bar{\omega}_{co}^2 u_t^2}{s\bar{\Omega}\bar{\omega}_o\gamma}h\right) e^{-i[\Lambda+\psi]}\right] + \bar{\omega}_o\left(1 - \frac{s\Omega}{\bar{\omega}_o\gamma}\right) \tag{14b}$$

$$\frac{du_z}{d\bar{z}} = \frac{u_t}{u_z\bar{\omega}_o} f J_s'(\bar{k}_t \bar{r}_L) Re\left[i\frac{dh}{d\bar{z}} e^{-i[\Lambda+\psi]}\right] \tag{14c}$$

where $u_t=\gamma v_t/c$ is the normalized transverse momentum amplitude, $u_z=\gamma v_z/c$ is the normalized axial momentum, Λ gives the slow

variation in the transverse momentum azimuthal phase relative to the reference wave phase, s is the harmonic number, γ is the relativistic mass ratio, k_t is the mode transverse wavenumber, r_L is the Larmor radius of the orbit, J_s (J_s') is (the derivative of) a regular Bessel function, Ω is the nonrelativistic cyclotron frequency, and f is the normalized rf field amplitude:

$$f = \frac{|e|}{m_o c^2} x'_{mn} C_{mn} J_{m-s}(k_t R_o)\, a \qquad (15)$$

Quantities with a "-" have been normalized according to: $\bar{z}=z/r_{wo}$, $\bar{r}_L=r_L/r_{wo}$, $\bar{\Omega}=\Omega r_{wo}/c$, $\bar{\omega}_o=\omega_o r_{wo}/c$, and $\bar{k}_n=k_n r_{wo}$. R_o denotes the orbit guiding center radius, e is the electron charge, m_o is the electron mass, m is the mode azimuthal index, x'_{mn} is a zero of J'_m, and r_{wo} is an arbitrary normalization factor. The transverse TE mode normalization coeficient

$$C_{mn} = \left[\sqrt{[\pi(x'^2_{mn}-m^2)]}\,J_m(x'_{mn})\right]^{-1} \qquad (16)$$

The ac current density is obtained by integrating Eqs.(14) for an appropriate set of initial conditions at the cavity input at z_o. For a cold, phase-mixed electron beam: $u_t(z_o)=u_{to}$, $u_z(z_o)=u_{zo}$, and $\Lambda(z_o)=\Lambda_o$ is uniformly distributed in the interval $[0,2\pi]$. For a thin annular beam the transverse ac current density is given by

$$J_t = -\frac{I_o}{v_z} v_t \qquad (17)$$

Substitution of Eqs.(17) and (6) into Eqs.(12) and using the prescription developed in previous work [7] leads to the following equations for the time-dependent wave and phase:

$$-4k_{z_o}A(t)\beta\sin[2k_{z_o}L-\psi(t)] + 2N\left[\frac{\omega_o^2-\omega_{r_o}^2}{c^2}\,a(t)^2 + 2\frac{\omega_o}{c^2}a(t)^2\dot{\psi}\right] = \tag{18a}$$

$$-4\mu_o I_o \omega_o C_{mn} J_{m-s}(k_t R_o)a(t)\int_0^L dz h(z)\left\langle\frac{\partial J_s(k_t r_L)}{\partial r_L}\,\frac{u_t}{u_z}\,\sin(\Lambda+\psi)\right\rangle_{\Lambda_o}$$

from Eq.(12a); and, from Eq.(12b),

$$2k_{z_o}[A(t)^2-\beta^2] + 4\frac{\omega_o}{c^2}a(t)\dot{a}(t)N =$$

$$4\mu_o I_o \omega_o C_{mn} J_{m-s}(k_t R_o)a(t)\int_0^L dz h(z)\left\langle\frac{\partial J_s(k_t r_L)u_t}{\partial r_L}\,\frac{}{u_z}\cos(\Lambda+\psi)\right\rangle_{\Lambda_o} \tag{18b}$$

where $\langle\ \rangle_a$ denotes an average with respect to the variable a. The cavity field amplitude can be related to the external field amplitude via the output diffraction Q factor according to:

$$A(t) = \sqrt{\frac{N}{k_{z_o}Q}}\,\frac{\omega_o}{c}\,a(t) \tag{19}$$

Substituting Eq.(19) into Eqs.(18), the equations for the time-dependent phase and amplitude can be written in the form:

$$\frac{d\psi}{d\tau} = -\frac{\Delta\omega_o}{\omega_o} - \frac{I}{f}\int_0^{\bar{L}} d\bar{z}\,h(\bar{z})\left\langle J_s'(\bar{k}_t\bar{r}_L)\,\frac{u_t}{u_z}\sin(\Lambda+\psi)\right\rangle_{\Lambda_o}$$

$$+\frac{1}{Q}\frac{f_L}{f}\sin[\psi-\Phi_o] \qquad (20a)$$

$$\frac{df}{d\tau} = -\frac{1}{2Q}\frac{f^2-f_L^2}{f} + I\int_0^{\bar{L}} d\bar{z}\,h(\bar{z})\left\langle J_s'(k_t r_L)\,\frac{u_t}{u_z}\cos(\Lambda+\psi)\right\rangle_{\Lambda_o} \qquad (20b)$$

where $\Delta\omega_o=\omega_o-\omega_{ro}$, $\Phi_o=k_{zo}L$, f_L is an effective field amplitude due to the locking signal given by:

$$f_L = \frac{|e|}{m_o c}\,x'_{mn}C_{mn}J_{m-s}(k_t R_o)\sqrt{\frac{2\mu_o Q P_L}{N\omega_o}} \qquad (21)$$

where P_L is the locking signal power, and I is the normalized current parameter:

$$I = \frac{|e|\mu_o}{m_o c\bar{\omega}_o}\,\frac{r_{wo}\,J_{m-s}^2(k_t R_o)}{\pi(1-m^2/x'^2_{mn})J_m^2(x'_{mn})N}\,I_o \qquad (22)$$

To treat the case of phase-locking via beam prebunching, the current density perturbation is assumed to be due to phase bunching. The ac current density perturbation can then be expressed in the form:

$$\hat{\delta J} \equiv \delta J_x + i\delta J_y = -I_o\frac{v_{to}}{v_{zo}}\,e^{-i(\omega_o t-\delta\Lambda)}\,\delta(r-R_o) \qquad (23)$$

where

$$\delta\Lambda = \frac{\omega_o - \Omega}{v_{zo}} z + \theta_o - q\sin\theta_o - \Phi_o \qquad (24)$$

where q is the bunching parameter and Φ_o is a phase factor determined by the locking signal. Evaluating the terms in Eqs.(9) involving δJ in the same manner as the terms involving J and using Eq.(23) leads to:

$$\frac{c^2\mu_o}{4N\omega_o a(t)^2}\int_V dadz\left[f^* e^* \cdot \delta J_\omega \stackrel{+}{-} fe \cdot \delta J_\omega^*\right] =$$

$$\begin{Bmatrix} -1 \\ -i \end{Bmatrix} \frac{I}{r_{wo} f} \frac{v_{to}}{v_{zo}} J_s'(k_t r_{Lo}) \int_o^L dz h(z) \left\langle \begin{Bmatrix} \cos \\ \sin \end{Bmatrix} (\delta\Lambda + \psi) \right\rangle_{\theta_o} \qquad (25)$$

where the "+" ("-") sign on the left hand side of Eq.(25) is associated with the upper (lower) quantities in the brackets on the right hand side. Substituting Eq.(24) into (25), and performing the phase average yields:

$$\frac{c^2\mu_o}{4N\omega_o a(t)^2}\int_V dadz\left[f^* e^* \cdot \delta J_\omega \stackrel{+}{-} fe \cdot \delta J_\omega^*\right] = \qquad (26)$$

$$\begin{Bmatrix} -1 \\ i \end{Bmatrix} \frac{I\ v_{to}}{r_{wo} f v_{zo}} J_s'(k_t r_{Lo}) \int_o^L dz h(z) J_1(q) \begin{Bmatrix} \sin \\ \cos \end{Bmatrix} \left(\frac{\omega_o - \Omega}{v_{zo}} z + \psi - \Phi_o\right)$$

Under the assumption of phase bunching only, the bunching parameter has no z-dependence in the cavity region and assuming a gaussian form for the profile function h(z), the axial integration can be carried out to obtain:

$$\frac{c^2\mu_o}{4N\omega_o a(t)^2}\int_V dadz\left[f^* e^* \cdot \delta J_\omega \pm f e \cdot \delta J_\omega^*\right] \approx \tag{27}$$

$$\begin{Bmatrix}-1\\ i\end{Bmatrix}\frac{\sqrt{\pi I}}{\kappa r_{w_o} f}\frac{v_{t_o}}{v_{z_o}}J_s'(k_t r_{L_o})e^{-\left[\frac{\omega_o-\Omega}{2v_{z_o}\kappa}\right]^2}J_1(q)\begin{Bmatrix}\sin\\ \cos\end{Bmatrix}(\psi-\Phi_o)$$

where the cavity axial wavenumber defines an effective interaction length according to $\kappa \equiv 2/L$. Substituting Eq.(27) into Eqs.(9) leads to the counterparts of Eqs.(20) for the case of phase-locking via a prebunched beam:

$$\frac{d\psi}{d\tau} = -\frac{\Delta\omega_o}{\omega_o} - \frac{I}{f}\int_0^L d\bar{z}h(\bar{z})\left\langle J_s'(\bar{k}_t\bar{r}_L)\frac{u_t}{u_z}\sin(\Lambda+\psi)\right\rangle_{\Lambda_o}$$
$$+\frac{\pi^3}{x_{mn}'}\frac{L}{\lambda}\frac{I}{f}\frac{v_{t_o}}{v_{z_o}}J_s'(k_t r_{L_o})e^{-\left[\frac{\omega_o-\Omega}{2v_{z_o}\kappa}\right]^2}J_1(q)\cos(\psi-\Phi_o) \tag{28a}$$

$$\frac{df}{d\tau} = -\frac{f}{2Q} + I\int_0^L d\bar{z}h(\bar{z})\left\langle J_s'(k_t r_L)\frac{u_t}{u_z}\cos(\Lambda+\psi)\right\rangle_{\Lambda_o}$$
$$+\frac{\pi^3}{x_{mn}'}\frac{L}{\lambda}I\frac{v_{t_o}}{v_{z_o}}J_s'(k_t r_{L_o})e^{-\left[\frac{\omega_o-\Omega}{2v_{z_o}\kappa}\right]^2}J_1(q)\sin(\psi-\Phi_o) \tag{28b}$$

Eqs.(28) have been derived in part to show the similar structure of the phase and amplitude equations for a gyrotron driven by a directly injected rf signal or by a premodulated beam. As discussed by Manheimer [16], these equations also lead to analytical estimates of the maximum frequency bandwidth for phase-locking, i.e., Adler's relation [Eq.(30) below], and of the exponentiation time in the approach to phase-lock. To carry out nonlinear numerical calculations of the temporal evolution of an oscillator driven by a premodulated beam it is more accurate to incorporate the beam premodulation directly into the wave equation source term via the initial conditions on the electron equations of motion. In this approach a nonuniform initial phase distribution is used of the form:

$$\Lambda_o = \theta_o - q\sin\theta_o - \Phi_o \tag{29}$$

where θ_o is uniformly distributed in the interval $[0,2\pi]$.

Eqs.(20) and (28) can be used to obtain estimates of the maximum frequency bandwidth for obtaining phase-locked operation for given system parameters. The wave amplitude and frequency shift due to beam loading for the free-running oscillator during steady-state operation are given by:

$$f_o = \left[2QI \int_0^L d\bar{z} h(\bar{z}) \left\langle J_s'(k_t r_L) \frac{u_t}{u_z} \cos(\Lambda+\psi) \right\rangle_{\Lambda_o} \right]_{ss} \tag{30a}$$

$$\frac{\Delta\omega_{FRO}}{\omega_o} = -\frac{I}{f_o}\left[\int_0^L d\bar{z}\,h(\bar{z})\left\langle J_s'(\bar{k}_t\bar{r}_L)\,\frac{u_t}{u_z}\sin(\Lambda+\psi)\right\rangle_{\Lambda_o}\right]_{ss} \qquad (30b)$$

where $\Delta\omega_{FRO}=\omega_{r1}-\omega_{ro}$ and ω_{r1} is the beam loaded resonant frequency of the free-running oscillator.

For an oscillator operating near steady-state conditions and driven by a weak external signal with frequency ω_o, Eqs.(30) can be used to rewrite Eq.(20a) as:

$$\frac{\partial\Psi}{\partial\tau} \simeq -\frac{\Delta\omega}{\omega_o} - \frac{1}{Q}\frac{f_L}{f_o}\sin(\Psi) \qquad (31)$$

where $\Delta\omega=\omega_o-\omega_{r1}$ and $\Psi=\psi-\Phi_o+\pi$. The condition for phase-locked operation, $\partial\Psi/\partial\tau=0$, implies:

$$\frac{\Delta\omega}{\omega_o} = -\frac{1}{Q}\frac{f_L}{f_o}\sin(\Psi_o) \qquad (32)$$

where Ψ_o denotes the phase during phase-locked operation. Since f_o and f_L are proportional to the square root of the oscillator output power and locking power, respectively, Eq.(32) leads to Adler's relation for the frequency pulling bandwidth of a phase-locked oscillator driving a matched load:

$$\frac{|\Delta\omega|}{\omega_o} \le \frac{1}{Q}\sqrt{\frac{P_L}{P_{ss}}} \qquad (33)$$

As discussed by Manheimer [16], for frequencies satisfying Eq.(33), Eq.(32) has a stable solution of the form: $\Psi=\Psi_o+\delta e^{-\tau/\Upsilon}$, where δ is a small perturbation, indicating that the approach to phase-locked operation is exponential. The time constant is given by:

$$\Upsilon = Q\sqrt{\frac{P_{osc}}{P_L}}\left[1 - \left(\frac{\Delta\omega Q}{\omega_o}\right)^2 \frac{P_{osc}}{P_L}\right]^{-1/2} \qquad (34)$$

Eq.(34) shows that Υ becomes large, and thus the time to achieve phase-lock becomes long, for frequencies near the bandwidth limit.

Similarly, in the case of phase-locking by beam pre-modulation, a similar analysis based on Eqs.(28) leads to the following equations describing the time-dependent amplitude and phase for operation near the oscillator steady-state:

$$\frac{d\Psi}{d\tau} \simeq -\frac{\Delta\omega}{\omega_o} - \frac{\sqrt{\pi}}{2}\frac{\mu I_G}{Q\ F} J_1(q)\ e^{-\left[\frac{\Delta\mu}{4}\right]^2}\left\{\frac{2^s s!}{s^s \beta_{t_o}^{s-1}} J_s'(s\beta_{t_o})\right\} \sin\Psi \qquad (35a)$$

$$\frac{dF}{d\tau} \simeq \frac{(F_o - F)}{2Q} + \frac{\sqrt{\pi}}{2}\frac{\mu I_G}{Q} J_1(q)\ e^{-\left[\frac{\Delta\mu}{4}\right]^2}\left\{\frac{2^s s!}{s^s \beta_{t_o}^{s-1}} J_s'(s\beta_{t_o})\right\} \cos\Psi \qquad (35b)$$

In deriving Eqs.(35) the following scaled "universal" gyrotron field amplitude, current, interaction length, and cyclotron resonance detuning parameters defined by Danly and Temkin [8] have been introduced:

$$F = \frac{\beta_{t\,o}^{s-4}}{\gamma_o}\left[\frac{s^s}{2^{s-1}\,s!}\right]\frac{f}{x'_{mn}} \tag{36a}$$

$$I_G = \left[\frac{2}{\pi}\right]^{\frac{3}{2}} \frac{Q\ \bar{\omega}_o}{\gamma_o\,\beta_{t\,o}^{2(3-s)}}\ \frac{N}{r_{w\,o}}\ \frac{\lambda}{L}\left[\frac{s}{2^s\,s!}\right]^2 I \tag{36b}$$

$$\mu = \pi\ \frac{\beta_{t\,o}^2}{\beta_{z\,o}}\ \frac{L}{\lambda} \tag{36c}$$

$$\Delta = \frac{2}{\beta_{t\,o}^2}\left(1 - \frac{s\Omega}{\omega_o}\right) \tag{36d}$$

The factor in Eqs.(35) involving the Bessel function $J'_s(s\beta_{t\,o})$ reduces to unity when the small argument expansion of the Bessel function is valid. This is a good approximation for weakly relativistic beams and low-order harmonic interactions but can lead to inaccuracies in the relativistic gyrotron regime of interest here. The condition for phase-locked operation, $\partial\Psi/\partial\tau=0$, implies:

$$\frac{\Delta\omega}{\omega_o} = -\frac{\sqrt{\pi}}{2}\frac{\mu I_G}{QF_{d\,o}}\,J_1(q)\ e^{-\left[\frac{\Delta\mu}{4}\right]^2}\left\{\frac{2^s\,s!}{s^s\,\beta_{t\,o}^{s-1}}\,J'_s(s\beta_{t\,o})\right\}\sin\Psi_o \tag{37}$$

where the amplitude of the driven oscillator F_{do} is given by:

$$F_{do} = F_o + \sqrt{\pi}\,\mu I_G\, J_1(q)\, e^{-\left[\frac{\Delta\mu}{4}\right]^2} \left\{\frac{2^s s!}{s^s \beta_{to}^{s-1}} J_s'(s\beta_{to})\right\} \cos\Psi_o \quad (38)$$

Eqs.(37) and (38) show that, unlike the case of direct injection, the amplitude of the driven oscillator has a dependence on the locking frequency. From the ratio of these equations one obtains: $(F_{do}-F_o)/F_{do}=2Q\cot\Psi_o\,\Delta\omega/\omega_o$ which shows that the change in wave amplitude can be of order Q times larger than the fractional frequency shift. Eq.(37) leads to the counterpart of Adler's relation for phase locking via a prebunched beam:

$$\frac{|\Delta\omega|}{\omega_o} \leq \frac{\sqrt{\pi}}{2}\frac{\mu I_G}{QF_{do}} J_1(q)\, e^{-\left[\frac{\Delta\mu}{4}\right]^2} \left\{\frac{2^s s!}{s^s \beta_{to}^{s-1}} J_s'(s\beta_{to})\right\} \quad (39)$$

A corresponding result was obtained by Manheimer[16] (using different notation) for the case of a gyrotron in a linearly polarized TE_{1n} mode. The time constant for the approach to phase-locked operation is given by:

$$\tau = \left[\frac{|\Delta\omega|^2_{max}}{\omega_o^2} - \frac{\Delta\omega^2}{\omega_o^2}\right]^{-1/2} \quad (40)$$

where $|\Delta\omega|_{max}/\omega_o$ is given by Eq.(39) with the equality sign.

Tran et al. [19] have used single-particle theory in the small signal approximation to calculate the bunching parameter q. Their result for the case of a single prebunching cavity with a gaussian axial field profile and circular mode polarization is:

$$q = \sqrt{\pi}\, F_1\, \mu_1\, e^{-\left[\frac{\Delta_1 \mu_1}{4}\right]^2} \left[\frac{\sqrt{3}}{2}\, \mu_1 + \mu_d\right] \tag{41}$$

where parameters with a "1" subscript denote bunching cavity parameters and μ_d is the normalized distance from the end of the bunching cavity to the beginning of the oscillator cavity.

III. CALCULATIONS AND RESULTS

Calculations have been carried out for a driven gyrotron oscillator using the theory developed in Section II. Phase locking by both direct injection and using a prebunching cavity has been simulated and the accuracy of simple theoretical estimates of locking bandwidth has been investigated. The dependence of the bandwidth for phase-locking on gyrotron operating parameters is shown.

The configuration analyzed is a high voltage 35 GHz gyrotron similar to the NRL experiment recently reported by Gold et al.[17]. The peak voltage and current of the annular beam are taken to be 650 kV and 1.5 kA, respectively, which are typical operating parameters. The beam guiding center radius is R_o=1.16 cm, the cavity radius is 1.6 cm, and the longitudinal profile of the cavity fields is assumed to be gaussian with effective length L=4 cm. The operating mode is the TE_{621} circular mode with polarization counter-rotating to the beam rotation. The beam pitch ratio $\alpha \equiv v_t/v_z = 1$. The cavity Q factor Q=250. Spreads in beam guiding center and pitch ratio are neglected as are space-charge effects. The cold cavity eigenfrequency for the TE_{621} mode is 35.08 GHz.

The calculated efficiency, output power and frequency shift due to beam loading of the free-running oscillator (FRO) are shown as a function of magnetic field in Figure 1. The corresponding transverse efficiency and normalized cavity wave amplitude are shown as a function of the detuning parameter Δ in

Figure 2. The electronic efficiency η is obtained from the transverse efficiency η_t according to: $\eta=\eta_t[\beta^2_{t_o}/2(1-\gamma_o^{-1})]$ where in the present case $\gamma_o=2.27$ and $\beta_{t_o}=0.63$. The transverse efficiency and normalized wave amplitude are related according to: $F^2=\eta_t I_G$. The normalized operating current is $I_G=0.238$. The normalized oscillation threshold current is also shown in Figure 2.

The case of direct injection of radiation is treated by integrating Eqs.(20). The injected locking power is taken to be 0.5 MW. The magnetic field is 2.5 Tesla [$\Delta=0.60$] and the cavity is seeded with a low amplitude field (E=1 kV/cm) at the beginning of the simulation. The time evolution of the driven oscillator output power is shown in Figure 3. This Figure shows that the steady state output power (140 MW) is achieved after about 5 nsec. The time evolutions of the driven oscillator frequency and phase are shown for three different locking frequencies in Figure 4. The oscillator frequency is expressed as the shift $\Delta\omega/\omega_o\equiv(\omega-\omega_o)/\omega_o\equiv d\psi/d\tau$ which vanishes when phase-locked operation is achieved. The initial locking frequency detuning $\Delta\omega_o/\omega_o\equiv(\omega_{FRO}-\omega_o)/\omega_o$ is 1×10^{-4}, 2×10^{-4}, and 3×10^{-4} in Figures 4(a), 4(b), and 4(c), respectively. According to Adler's relation [Eq.(33)], the maximum locking frequency shift for this magnetic field is $|\Delta\omega_o|_{max}/\omega_o=2.4\times10^{-4}$. As expected, the oscillator evolves toward phase-locked operation in Figures 4(a) and 4(b), whereas phase-locked operation is not obtained in Figure 4(c). Comparison of Figures 3 and 4 shows that the time to achieve the equilibrium phase during phase-locked operation is

much longer than the output power risetime. This confirms the validity of the assumptions made in obtaining Eq.(31) which in turn leads to Adler's relation.

The dependence of the phase angle for phase-locked operation on the locking frequency shift is shown in Figure 5 for the same oscillator parameters and locking power as above. The solid curve shows the analytical theory result [Eq.(32)] and the open circles indicate the results of slow-time-scale (STS) simulations. The angles plotted in Figure 5 correspond to the difference between the code result at each frequency shift and the code result for driving the oscillator at the free-running oscillator frequency. The dashed vertical lines indicate the minimum locking frequency shift for which phase-locked operation could not be obtained. This shift is found to be in good agreement with the maximum frequency shift predicted by Eq.(33),i.e., Adler's relation. Similar agreement was obtained between time-dependent calculations and Eq.(32) for a magnetic field of 2.4 Tesla. Since the oscillator is in the hard excitation regime for this magnetic field ($I<I_{thr}$), the cavity was seeded with the steady-state field amplitude in the time-dependent calculations. The phase-locking bandwidth for direct injection as a function of detuning parameter calculated using Eq.(32) is shown in Figure 6. This Figure shows that the bandwidth is insensitive to the interaction detuning.

Phase-angle vs. locking frequency shift results for a gyrotron oscillator driven via a prebunching cavity are shown in Figure 7. The solid curve is based on Eq.(37) and the open

squares are the results of integrating Eqs.(28) which are based on the perturbation theory (PT) approach. The open circles show results based on the klystron (K) approach in which the last terms on the right-hand-side (RHS) of Eqs.(28) are omitted and the beam phase bunching is introduced as initial conditions for the beam equations-of-motion. This avoids the approximation of separating the ac current density into two terms [cf. Eq.(4)]. The effect of the prebunching cavity, assuming phase bunching only, is represented by the bunching parameter q=0.16. This choice for q was used so the locking bandwidth prediction based on Eq.(39) for a magnetic field of 2.5 Tesla is the same as the direct injection result using 0.5 MW locking power. The time-dependent calculations based on perturbation theory are in good agreement with the results based on Eq.(37) except for negative frequency shifts near the bandwidth limit. The locking bandwidth obtained from the simulations is about 8% less than the result obtained using Eq.(39) which is considered to be good agreement considering the complexity of the time-dependent calculations. On the other hand the locking bandwidth obtained from simulations using the klystron approach is about 80% wider than the result obtained from Eq.(39) for this magnetic field. This difference is attributed to the approximation inherent in the perturbation theory approach.

The effect on the locking bandwidth of varying the magnetic field detuning parameter is shown in Figure 8 for phase-locking using a prebunched beam. According to Eq.(39) the locking bandwidth based on perturbation theory decreases rapidly as the

detuning is increased. This behavior is shown in Figure 8 and implies a constraint on efficiency optimization. The decrease in bandwidth with increase in Δ obtained from simulations based on the klystron method is less pronounced than the perturbation theory results. The results of the two approaches converge and finally cross as the detuning is decreased. Comparison of Figures 6 and 8 shows a much stronger dependence on detuning parameter for phase locking with a prebunching cavity than by direct injection which is essentially independent of the detuning parameter. Figure 8 also shows the dependence of the exponentiation time constant, given in dimensionless form by Eq.(40), for the approach to phase-locked operation on the detuning parameter. The time constant plotted in Figure 8 corresponds to a locking frequency shift of one half the maximum frequency shift for obtaining phase-locked operation. To obtain the time constant in seconds, the result given by Eq.(40) should be divided by the operating frequency. Figure 8 shows that for the present configuration operating at 35 GHz and Δ=0.6 the e-folding time is 21 nsec for a bunching parameter of 0.16. This time can be decreased to a few nanoseconds by increasing the bunching parameter and decreasing the detuning parameter.

IV. DISCUSSION AND CONCLUSIONS

The extension of slow-time-scale steady-state gyrotron theory to time-dependent analysis of gyrotron oscillators driven by an external signal is demonstrated in this work. Calculations based on this theory yield the time evolution of the driven oscillator output frequency and phase for either the approach to phase-locked operation or for unphase-locked operation. These results should facilitate the investigation of driven intense-beam gyrotrons which are characterized by short pulselengths.

In the case of phase locking by direct injection, the maximum locking frequency shift which allows phase-locked operation obtained by integrating the STS time-dependent equations for the radiation amplitude and phase is in good agreement with Adler's relation. The simulations demonstrate the validity of the conceptual model which treats the phase-locking process as a perturbation of the free-running oscillator operation. Such calculations for frequencies near the maximum allowed frequency shift are costly since the time constant for the exponential approach to the phase-locked equilibrium phase becomes large in this limit. An important objective in carrying out the calculations shown, for example, in Figure 5 was to establish the time and space increments and number of phases needed to obtain accurate results from the time-dependent simulations.

In the case of phase locking using a prebunching cavity, the time-dependent calculations show that the perturbation theory approach underestimates the frequency shift bandwidth for phase

locking except at small detuning parameters. The analytical bandwidth estimates based on the perturbation theory approach are nevertheless extremely useful for design purposes. The generality of the results has been increased by expressing the results in terms of well-known dimensionless gyrotron parameters. The present results for a circularly polarized mode also extend the results obtained previously by Manheimer for a TE_{1n} linearly polarized mode.

A few comments can be made regarding the maximum obtainable bandwidth using a prebunching cavity. According to the perturbation theory approach, the maximum bandwidth is obtained when the bunching parameter $q=1.83$ since this maximizes the Bessel function $J_1(1.83)=0.58$. Based on the results of this paper, nonlinear, nonperturbation theory calculations should yield somewhat larger bandwidth for a given bunching parameter. A bunching parameter $q>1.83$ should also lead to larger bandwidth when nonlinear effects are taken into account. However, in practice, as discussed below, $q\geq 2$ is difficult to obtain so that the maximum bandwidth based on perturbation theory represents a reasonable estimate of achievable bandwidth.

To increase the generality of the results it is convenient to neglect the term in curly brackets on the right hand side of Eq.(39). This leads to an error of 15% for the high voltage, fundamental interaction configuration analyzed in this paper. The error is much less for lower voltage (~100 kV) configurations except for high harmonic interactions. In this approximation the maximum bandwidth depends only on the resonator Q factor, the

normalized steady-state resonator RF field amplitude F_o, the interaction length μ, the beam current parameter I_G, and the resonance detuning parameter Δ. Thus, in principle, the phase-locking bandwidth associated with beam premodulation method does not depend on the power of the locking signal because by suitable bunching cavity and drift tube design a large bunching parameter can be obtained with a small input signal. In practice, of course, this is a difficult problem, especially for overmoded systems.

The normalized gyrotron parameters corresponding to efficient operation are highly constrained. Since, for steady-state operation $I_G = F_o^2/\eta_t$, the estimate for Q times the maximum bandwidth depends only on F_o, μ, and Δ; and is given by:

$$Q\,\frac{|\Delta\omega|}{\omega_o} \leq 0.5\,\frac{\mu F_o}{\eta_t(F_o,\mu,\Delta)}\,e^{-\left[\frac{\Delta\mu}{4}\right]^2} \qquad (42)$$

The transverse efficiency for given F_o, μ, and optimized Δ can be obtained from an F-μ plot [8] when the electron dynamics are treated according to the "generalized pendulum" equations of motion. The parameters yielding the optimum transverse efficiency of $\eta_t \sim 0.7$ are approximately $\mu=15$, $F_o=0.15$, and $\Delta=0.5$. These parameters are typical of thermionic cathode gyrotrons developed for average power applications [20] and, for Q=250, Eq.(42) leads to a maximum bandwidth for phase locking with a prebunching cavity of $|\omega|/\omega_o = 0.02\%$. According to Adler's

Relation, to obtain this bandwidth using direct injection, a locking power to oscillator power ratio of P_L/P_{out}=-26.4 dB is required, i.e. 2.2 kW would be required to obtain this phase-locking bandwidth for a state-of-the-art megawatt gyrotron using direct injection. Presumably much less locking power would be required for the beam permodulation method with a well designed bunching cavity system. On the other hand if more locking power is available, then wider bandwidth can be obtained using direct injection. Thus, from this point of view, which does take into account many important practical considerations, phase locking using a prebunching cavity appears more effective for systems which are locking power limited whereas systems with ample locking power can achieve wider bandwidth by employing direct injection.

Representative normalized parameters for the high peak power configuration analyzed in this work are F_o=0.33, μ=9.2, Δ=0.7, and η_t=0.45. These parameters lead to a maximum phase-locking bandwidth of $|\omega|/\omega_o$=0.1% for Q=250 and a corresponding phase-locking power ratio of P_L/P_{out}=-11.9 dB. Thus, the use of the beam prebunching method appears to be particularly advantageous for high peak power gyrotrons which are characterized by high cavity RF fields and short interaction lengths. This is because of the wider bandwidth achievable in this regime, and because these devices are likely to be locking power limited.

Aside from the bandwidth potential of the beam premodulation method it also has the advantage of isolating the oscillator output from the locking source. However, multiple bunching

cavities will generally be required to realize the maximum bandwidth potential with low power. To prevent self-oscillation the bunching cavities are usually short with $\mu_B \sim 2$ being a typical value. The Q factor should low for the same reason, i.e. $Q_B \sim 200$. For a low drive power this leads to a RF field amplitude in the first bunching cavity which is at least an order of magnitude less than the output cavity field, i.e. $F_{B1} \sim F_o/10 \sim 0.03$. Finally, the drift section should be short to prevent degradation of the phase bunching due to beam velocity spread with $\mu_d \sim 3$ being a typical value. In the absence of significant magnetic field tapering, the bunching cavity detuning parameter is the same as in the output cavity. Substituting these parameters into Eq.(41) leads to a rough estimate of the bunching parameter obtainable from a single bunching cavity, that is, $q \sim 0.4$, which is much less the value assumed in the estimate of the maximum bandwidth. This estimate has been confirmed by more detailed calculations [21]. To increase the bunching additional passive bunching cavities can be used. The design of a multicavity phase-locked gyrotron is discussed in Ref. 21.

V. ACKNOWLEDGEMENTS

Helpful discussions with Drs. Steven Gold, Ed Ott, and John Burke are gratefully acknowledged as is the computational assistance of Robert Lee. This work was sponsored by the Office of Innovative Science and Technology of the Strategic Defense Initiative Organization and was managed by the Harry Diamond Laboratory. The computer time for the numerical calculations was funded by the Naval Research Laboratory 6.1 Cray Production Run Program.

REFERENCES

1. P. Sprangle and W.M. Manheimer, Phys. Fluids 18, 224 (1975).
2. E. Ott and W.M. Manheimer, IEEE Trans. Plasma Sci. PS-13, 1 (1975).
3. V.A. Flyagin, A.V. Gaponov, A.V. Petelin, and V.K.Yulpatov, IEEE Trans. Microwave Theory Tech. MTT-25, 514 (1977).
4. P. Sprangle and A.T. Drobot, IEEE Trans. Microwave Theory Tech. MTT-25, 528 (1978).
5. K.R. Chu, Phys. Fluids 21, 2354 (1978).
6. K.R. Chu, A.T. Drobot, H.H. Szu, and P. Sprangle, IEEE Trans. Microwave Theory Tech. MTT-28, 313 (1980).
7. A.W. Fliflet, M.E. Read, K.R. Chu, and R. Seeley, Int. J. Electron. 53, 505 (1982).
8. B.G. Danly and R.J. Temkin, Phys. Fluids 29, 561 (1986).
9. R. Adler, Proc. Inst. Radio Engrs. 34, 351 (1946).
10. M. Caplan, A.T. Lin, and K.R. Chu, Int. J. Electron. 53, 659 (1982).
11. M.A. Moiseev and G.S. Nusinovich, Isvestia VUZ. Radiofizika 17, 1709 (1974) [Radio Phys. Quant. Electron. 17, 1305 (1976)].
12. N.S. Ginzburg, G.S. Nusinovich, and N.A. Zavolsky, Int. J. Electron. 61, 881 (1986).
13. A. Bondeson, W.M. Manheimer, and E. Ott, Phys. FLuids 26, 285 (1983).
14. B. van der Pol, Phil. Mag. 3, 65 (1927).
15. M.E. Read, R. Seeley, and W.M. Manheimer, IEEE Trans. Plasma Sci. PS-13, 398 (1985).
16. W.M. Manheimer, Int. J. Electron. 63, 29-47 (1987).

17. S.H. Gold, A.W. Fliflet, W.M. Manheimer, R.B. McCowan, W.M. Black, R.C. Lee, V.L. Granatstein, A.K. Kinkead, D.L. Hardesty, and M. Sucy, Phys. Fluids 30, 2226-2238 (1987).

18. A.W. Fliflet, Int. J. Electron. 61, 1049 (1986).

19. T.M. Tran, B.G. Danly, K.E.Kreischer, J.B. Schutkeker, and R.J. Temkin, Phys. Fluids 29, 1274 (1986)

20. K.E. Kreischer, B.G. Danly, J.B. Schutkeker, and R.J. Temkin, IEEE Trans. Plasma Sc. PS-13, 364 (1985).

21. A.W. Fliflet and S.H. Gold, NRL Memorandum Report 6065 (1987).

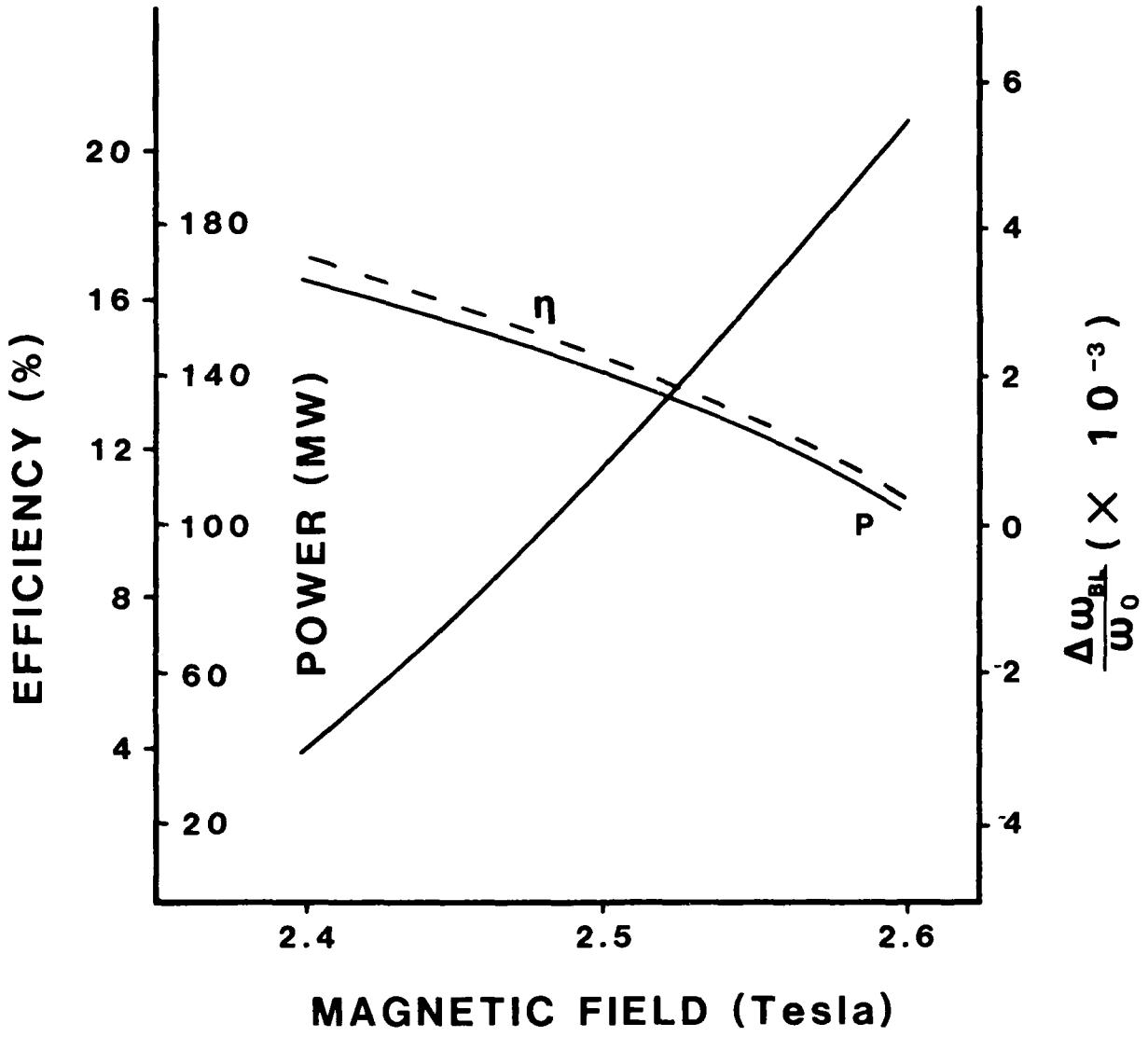

Figure 1: Efficiency, output power, and frequency shift due to beam loading for the free-running oscillator as a function of magnetic field.

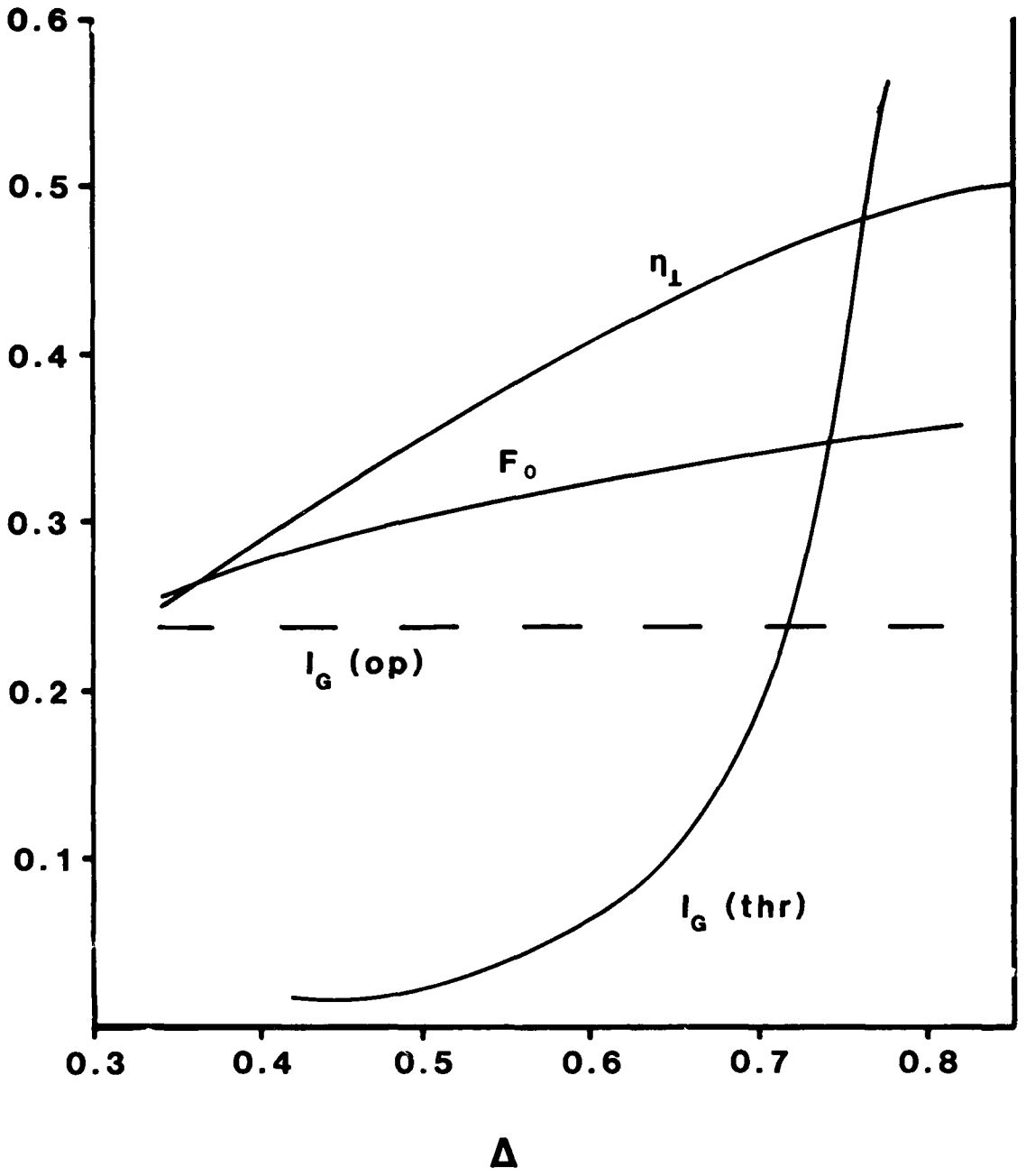

Figure 2: Normalized operating parameters for the free-running oscillator.

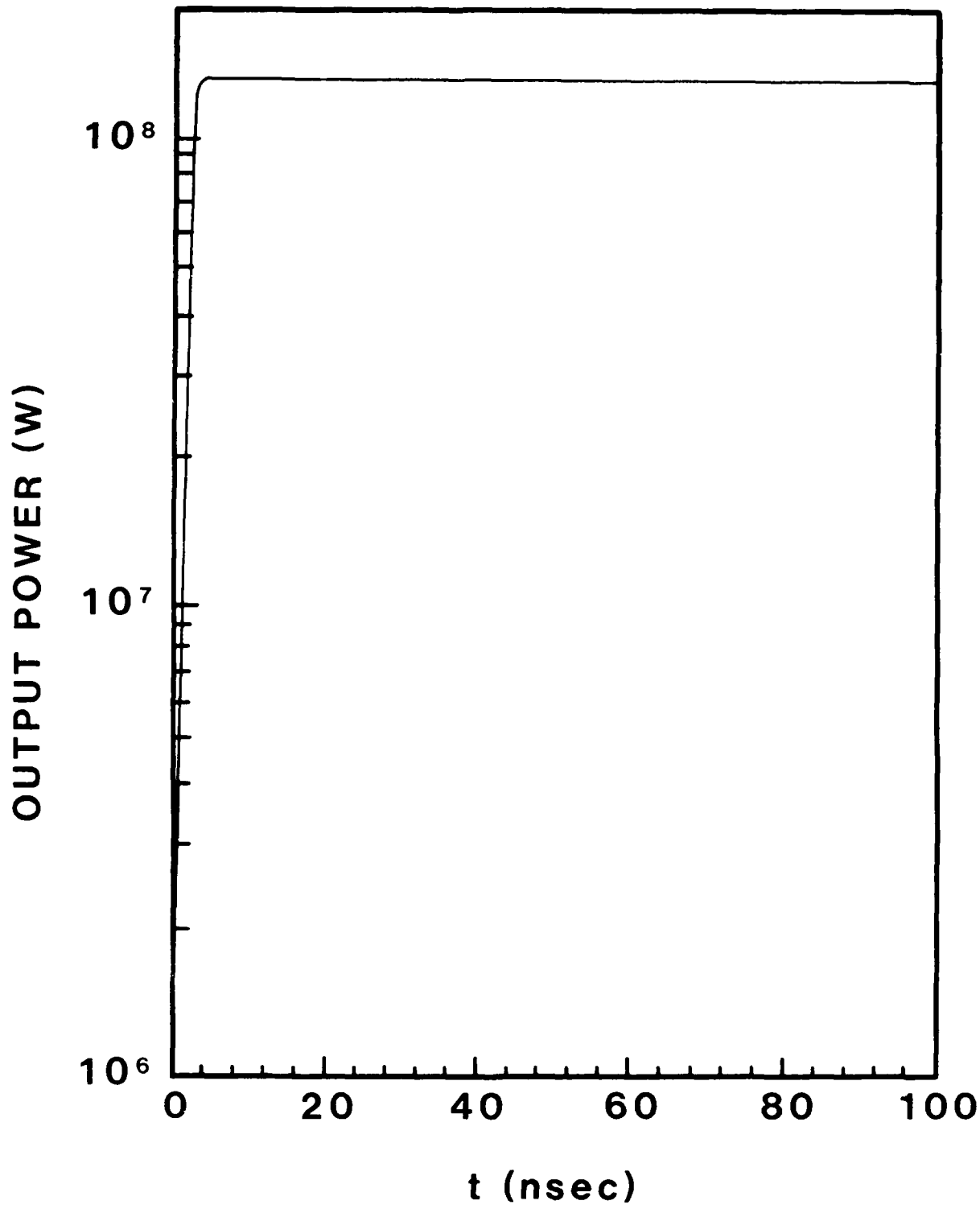

Figure 3: Time evolution of the output power of the oscillator driven by 0.5 MW directly injected signal. The locking frequency detuning is 7 MHz and the magnetic field is 25 kG.

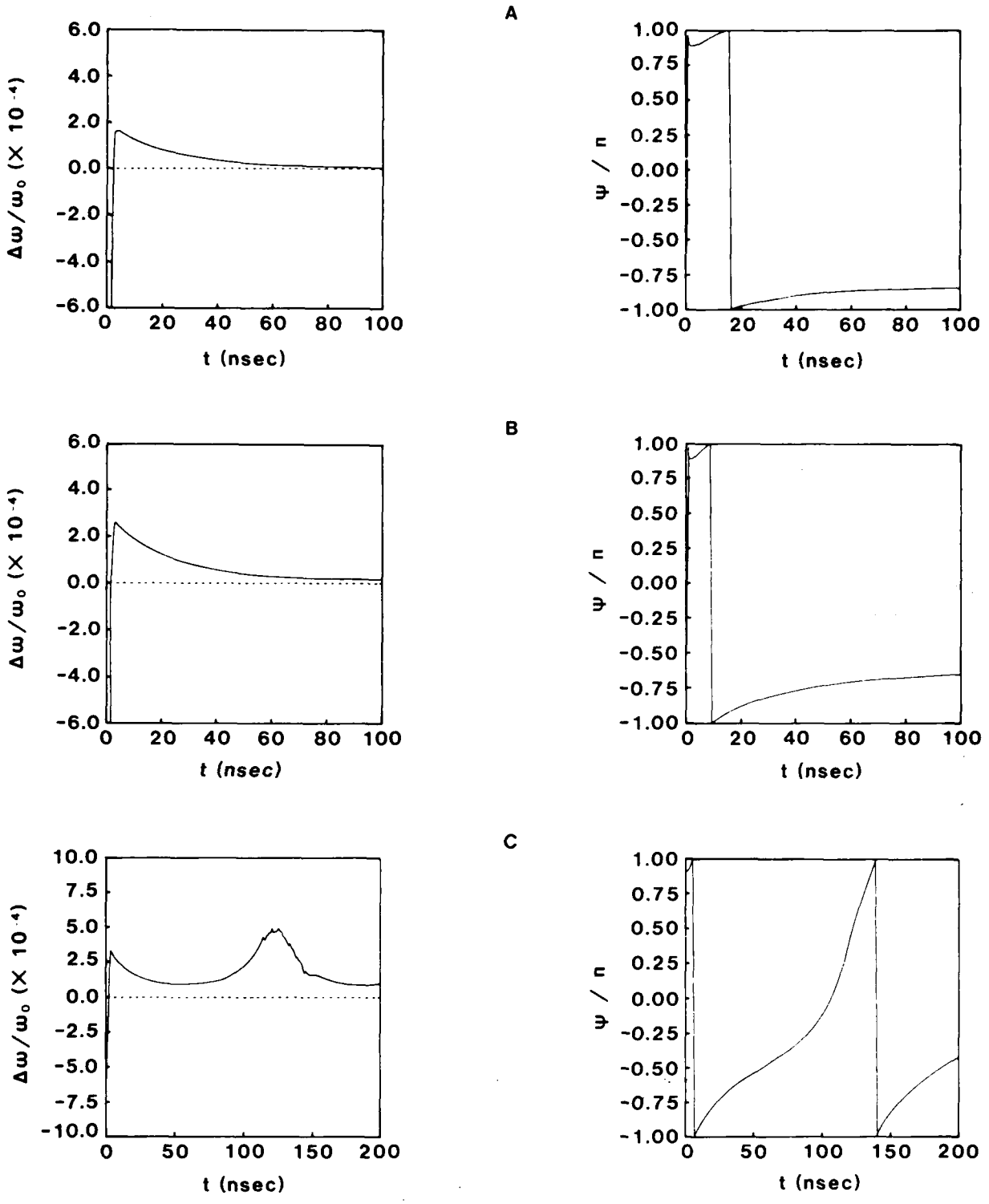

Figure 4: Time evolution of the frequency and phase of the driven oscillator for three locking frequency detunings, (a): 3.5 MHz, (b): 7 Mhz, (c): 10.5 MHz. Operating parameters are the same as for Figure 3.

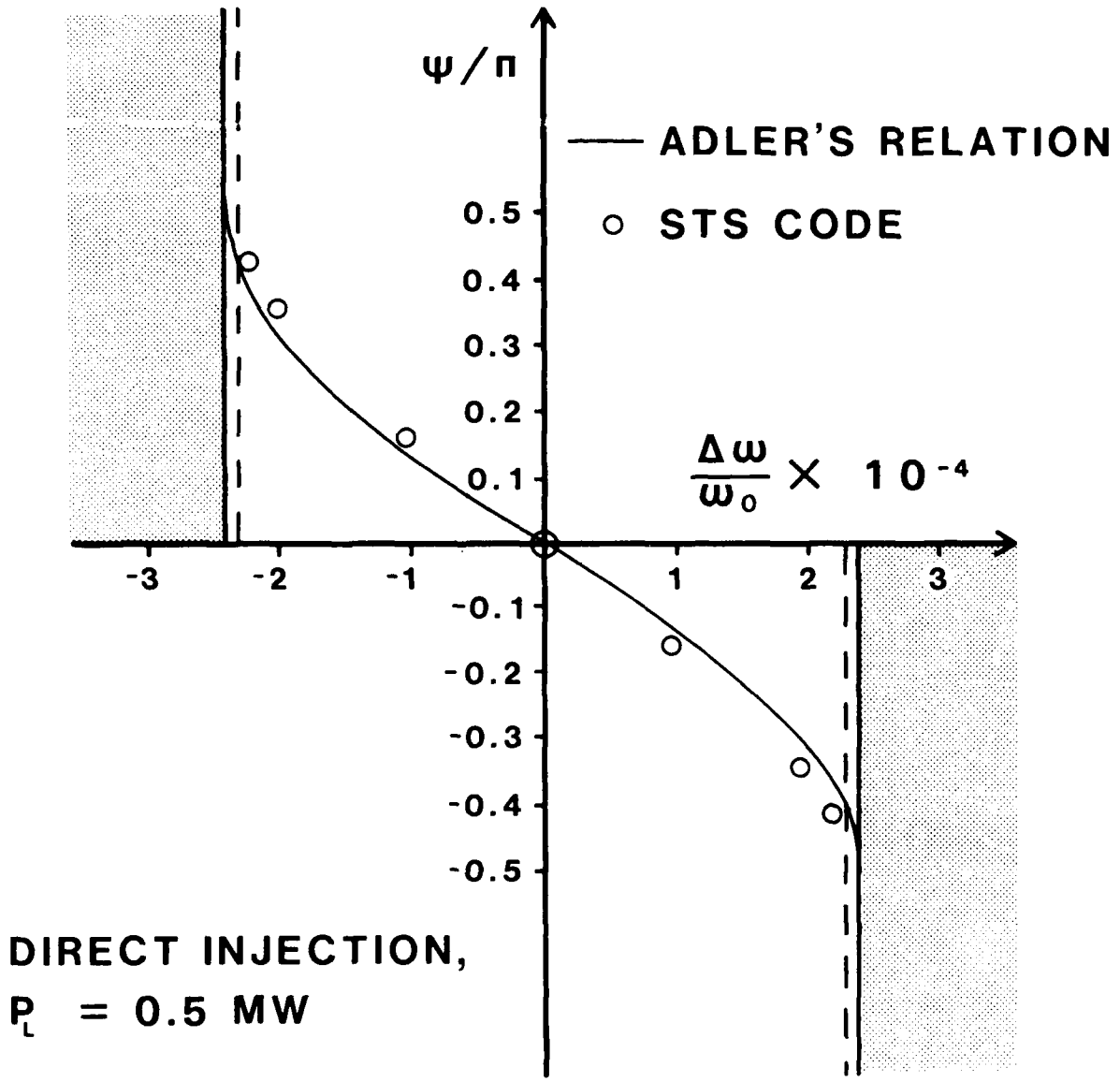

Figure 5: Equilibrium phase angle versus frequency shift for the oscillator driven by 0.5 MW directly injected signal. Solid curve: analytical theory, circles: time-dependent simulation results. Shaded regions: Locking frequencies excluded by Adler's relation, dashed lines: upper and lower bounds for locking bandwidth from time-dependent simulations.

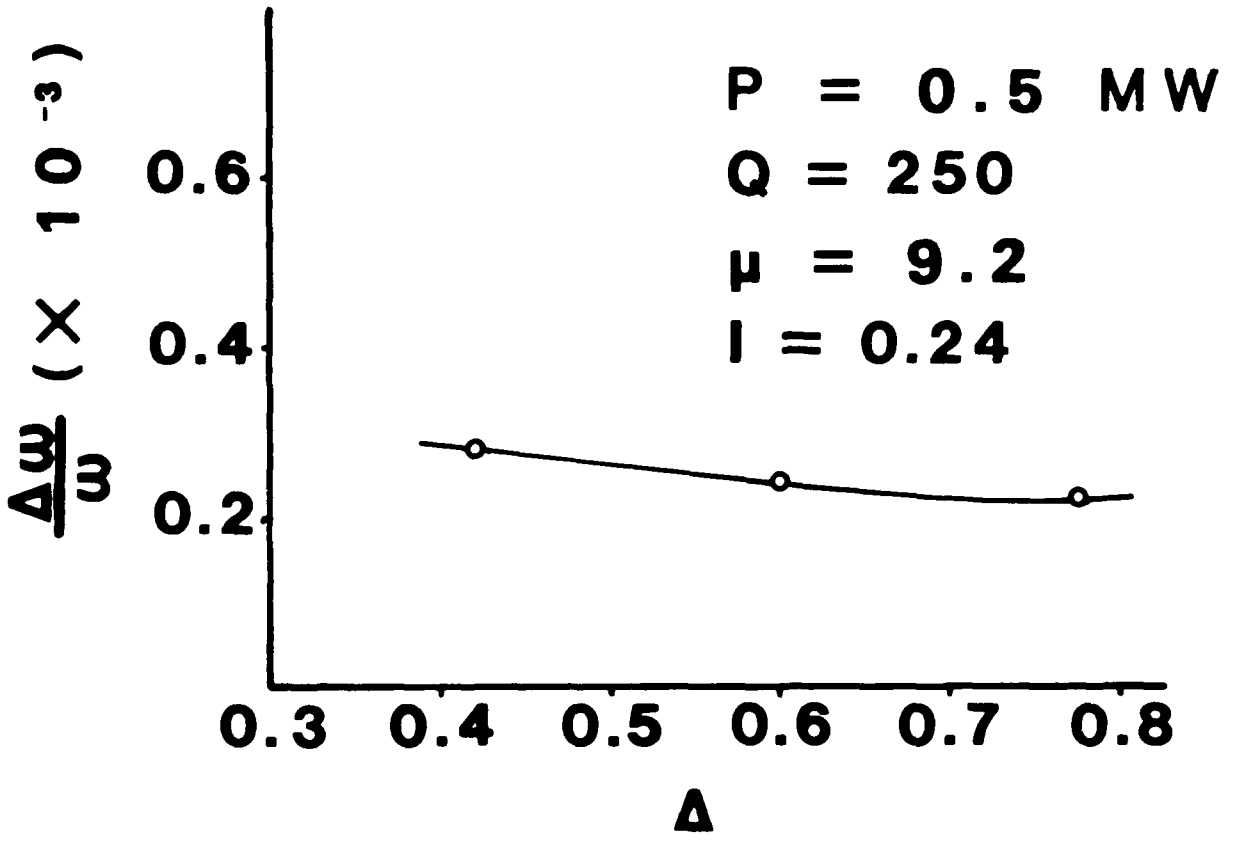

Figure 6: Phase-locking bandwidth as a function of detuning parameter for the oscillator driven by 0.5 MW directly injected signal.

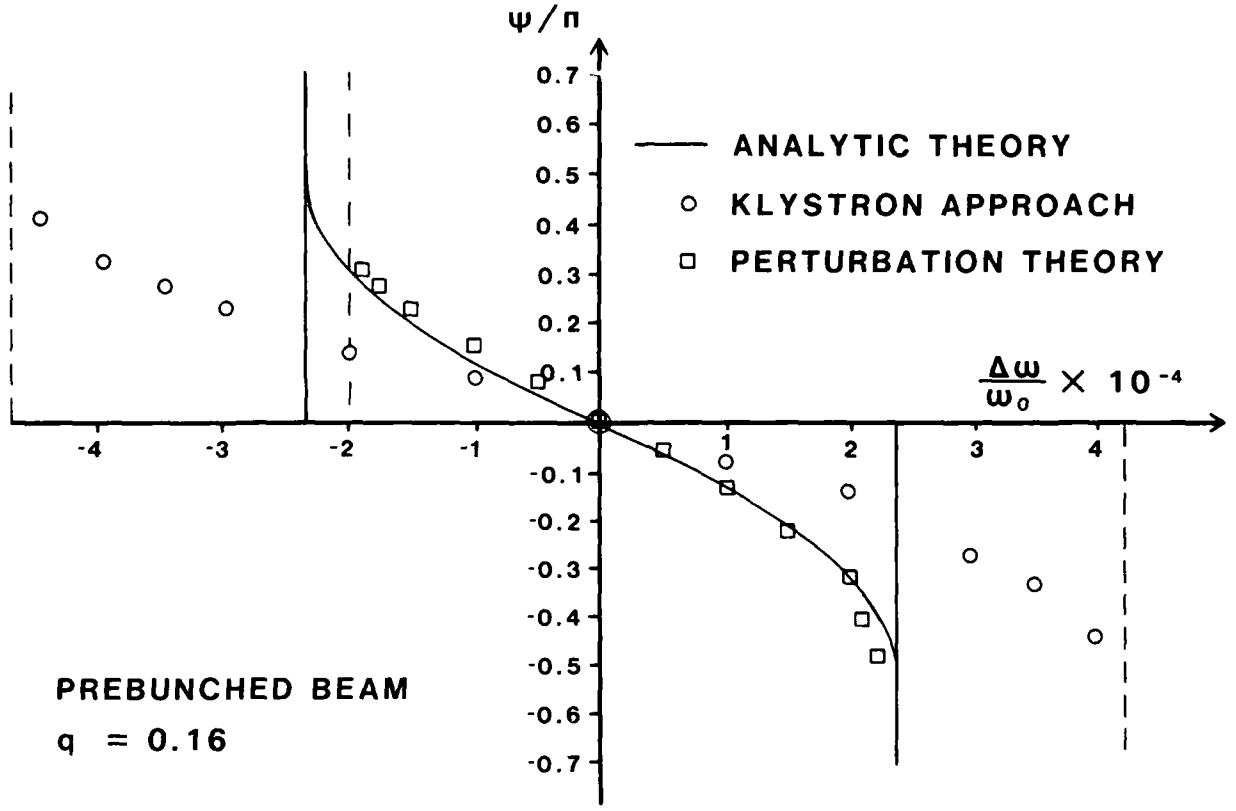

Figure 7: Equilibrium phase angle versus frequency shift for the oscillator driven by prebunched beam with q=0.16. Solid curve: analytical theory, squares: time-dependent simulation results based on perturbation theory, circles: time-dependent simulation results based on klystron theory. Dashed line: upper and lower bounds for locking bandwidth based on klystron approach, solid vertical lines: maximum bandwidth based on analytical perturbation theory, dash-dot-dash line: lower bound for locking bandwidth from time-dependent simulations based on perturbation theory.

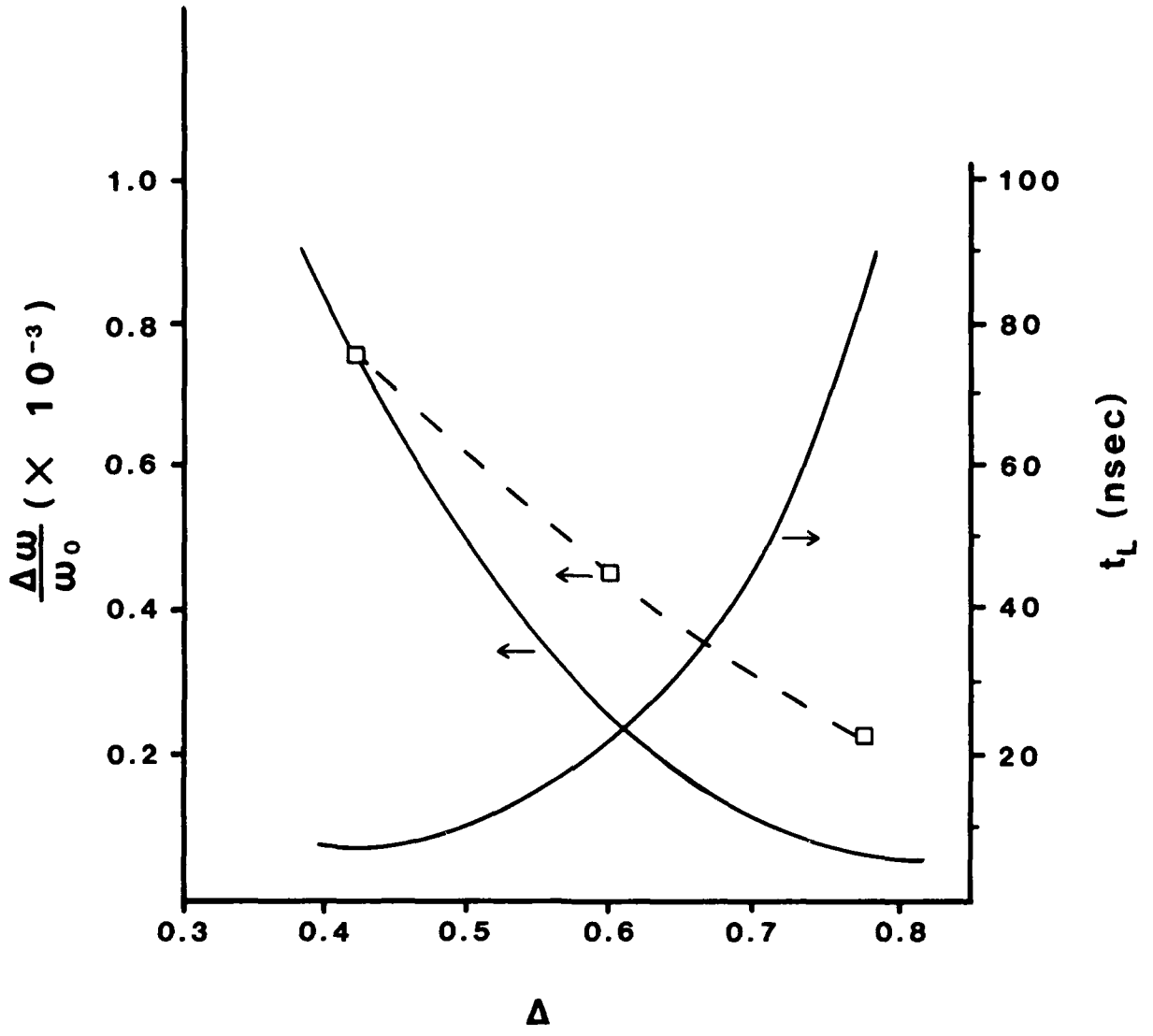

Figure 8: Phase-locking bandwidth as a function of detuning parameter for the oscillator driven by a prebunched beam with q=0.16. Solid curve associated with left hand axis: perturbation theory result, dashed curve: klystron approach result, solid curve associated with right hand axis: exponentiation time constant based on perturbation theory.

4740 DISTRIBUTION LIST

Air Force Avionics Laboratory
AFWAL/AADM-1
Wright/Patterson AFB, Ohio 45433
Attn: Walter Friez — 1 copy

Air Force Office of
Scientific Research
Bolling AFB
Washington, D.C. 20332
Attn: H. Schlossberg — 1 copy

Air Force Weapons Lab
Kirkland AFB
Albuquerque, New Mexico 87117
Attn: Dr. William Baker — 2 copy

Case Western Reserve University
Electrical Engineering & Applied
Physics Department
Cleveland, OH 44106
ATTN: Altan M. Ferendeci — 1 copy

Columbia University
520 West 120th Street
Department of Electrical Engineering
New York, N.Y. 10027
Attn: Dr. S.P. Schlesinger — 1 copy
A. Sen

Columbia University
520 West 120th Street
Department of Applied Physics
and Nuclear Engineering
New York, New York 10027
Attn: T.C. Marshall — 1 copy
R. Gross

Cornell University
School of Applied and Engineering Physics
Ithica, New York 14853
Attn: Prof. Hans H. Fleischmann — 1 copy
John Nation — 1 copy
R. N. Sudan — 1 copy

Dartmouth College
18 Wilder, Box 6127
Hanover, New Hampshire 03755
Attn: Dr. John E. Walsh — 1 copy

Department of Energy
Washington, D.C. 20545
Attn: C. Finfgeld/ER-542, GTN — 1 copy
T.V. George/ER-531, GTN — 1 copy
D. Crandall/ER-55, GTN — 1 copy
D. Beard/ER-531, GTN — 1 copy

Defense Advanced Research Project Agency/DEO
1400 Wilson Blvd.
Arlington, Virginia 22209
Attn: Dr. S. Shey — 1 copy
Dr. L. Buchanan — 1 copy

Defense Communications Agency
Washington, D.C. 20305
Attn: Dr. Pravin C. Jain
Assistant for Communications
Technology — 1 copy

Defense Nuclear Agency
Washington, D.C. 20305
Attn: Mr. J. Farber — 1 copy
Mr. Lloyd Stossell — 1 copy

Defense Technical Information Center
Cameron Station
5010 Duke Street
Alexandria, Virginia 22314 — 2 copies

Georgia Tech. EES-EOD
Baker Building
Atlanta, Georgia 30332
Attn: Dr. James J. Gallagher — 1 copy

Hanscomb Air Force Base
Stop 21, Massachusetts 01731
Attn: Lt. Rich Nielson/ESD/INK — 1 copy

Hughes Aircraft Co.
Electron Dynamics Division
3100 West Lomita Boulevard
Torrance, California 90509
Attn: J. Christiansen — 1 copy
J.J. Tancredi — 1 copy

KMS Fusion, Inc.
3941 Research Park Dr.
P.O. Box 1567
Ann Arbor, Michigan 48106
Attn: S.B. Segall — 1 copy

Lawrence Livermore National Laboratory
P.O. Box 808
Livermore, California 94550
Attn: Dr. D. Prosnitz — 1 copy
Dr. T.J. Orzechowski — 1 copy
Dr. J. Chase — 1 copy
Dr. M. Caplan — 1 copy

Los Alamos Scientific Laboratory
P.O. Box 1663, AT5-827
Los Alamos, New Mexico 87545
Attn: Dr. J.C. Goldstein — 1 copy

Dr. T.J.T. Kwan	1 copy
Dr. L. Thode	1 copy
Dr. C. Brau	1 copy
Dr. R. R. Bartsch	1 copy

Massachusetts Institute of Technology
Department of Physics
Cambridge, Massachusetts 02139

Attn: Dr. G. Bekefi/36-213	1 copy
Dr. M. Porkolab/NW 36-213	1 copy
Dr. R. Davidson/NW 16-206	1 copy
Dr. A. Bers/NW 38-260	1 copy
Dr. K. Kreischer	1 copy

Massachusetts Institute of Technology
167 Albany St., N.W. 16-200
Cambridge, Massachusetts 02139

Attn: Dr. R. Temkin/NW 14-4107	1 copy
Dr. B. Danley	1 copy

Spectra Technologies
2755 Northup Way
Bellevue, Washington 98004

Attn: Dr. J.M. Slater	1 copy

Mission Research Corporation
Suite 201
5503 Cherokee Avenue
Alexandria, Virginia 22312

Attn: Dr. M. Bollen	1 copy
Dr. Tom Hargreaves	1 copy

Mission Research Corporation
1720 Randolph Road, S.E.
Albuquerque, New Mexico 87106

Attn: Dr. Ken Busby	1 copy
Mr. Brendan B. Godfrey	1 copy

SPAWAR
Washington, D.C. 20363

Attn: E. Warden	
Code PDE 106-3113	1 copy
G. Bates	
PMW 145	1 copy

Naval Research Laboratory

Addressee: Attn: Name/Code	
Code 1001 - T. Coffey	1 copy
Code 1220 - Security	1 copy
Code 2628 - TID Distribution	22 copies
Code 4000 - W. Ellis	1 copy
Code 4600 - D. Nagel	1 copy
Code 4700 - S. Ossakow	26 copies
Code 4700.1 - A.W. Ali	1 copy
Code 4710 - C. Kapetanakos	1 copy
Code 4740 - Branch Office	25 copies
Code 4740 - W. Black	1 copy

Code 4740 - A. Fliflet	1 copy
Code 4740 - S. Gold	1 copy
Code 4740 - A. Kinkead	1 copy
Code 4740 - W.M. Manheimer	1 copy
Code 4740 - M. Rhinewine	1 copy
Code 4770 - G. Cooperstein	1 copy
Code 4790 - B. Hui	1 copy
Code 4790 - C.M. Hui	1 copy
Code 4790 - Y.Y. Lau	1 copy
Code 4790 - P. Sprangle	1 copy
Code 5700 - J. Montgomery	1 copy
Code 6840 - S.Y. Ahn	1 copy
Code 6840 - A. Ganguly	1 copy
Code 6840 - R.K. Parker	1 copy
Code 6840 - N.R. Vanderplaats	1 copy
Code 6850 - L.R. Whicker	1 copy
Code 6875 - R. Wagner	1 copy

Northrop Corporation
Defense Systems Division
600 Hicks Rd.
Rolling Meadows, Illinois 60008
Attn: Dr. Gunter Dohler — 1 copy

Oak Ridge National Laboratory
P.O. Box Y
Mail Stop 3
Building 9201-2
Oak Ridge, Tennessee 37830
Attn: Dr. A. England — 1 copy

Office of Naval Research
800 N. Quincy Street
Arlington, Va. 22217
Attn: Dr. C. Roberson — 1 copy
Dr. W. Condell — 1 copy
Dr. T. Berlincourt — 1 copy

Office of Naval Research
1030 E. Green Street
Pasadena, CA 91106
Attn: Dr. R. Behringer — 1 copy

Optical Sciences Center
University of Arizona
Tucson, Arizona 85721
Attn: Dr. Willis E. Lamb, Jr. — 1 copy

OSD/SDIO
Attn: IST (Dr. H. Brandt)
Washington, D.C. 20301-7100 — 1 copy

Pacific Missile Test Center
Code 0141-5
Point Muga, California 93042
Attn: Will E. Chandler — 1 copy

Physical Dynamics, Inc.
P.O. Box 10367
Oakland, California 94610
Attn: A. Thomson — 1 copy

Physics International
2700 Merced Street
San Leandro, California 94577
Attn: Dr. J. Benford — 1 copy

Physical Science Inc.
603 King Street
Alexandria, VA 22314
ATTN: M. Read — 1 copy

Princeton Plasma
Plasma Physics Laboratory
James Forrestal Campus
P.O. Box 451
Princeton, New Jersey 08544
Attn: Dr. H. Hsuan — 2 copies
Dr. J. Doane — 1 copy
Dr. D. Ignat — 1 copy
Dr. H. Furth — 1 copy
Dr. P. Efthimion — 1 copy
Dr. F. Perkins — 1 copy

Quantum Institute
University of California
Santa Barbara, California 93106
Attn: Dr. L. Elias — 1 copy

Raytheon Company
Microwave Power Tube Division
Foundry Avenue
Waltham, Massachusetts 02154
Attn: N. Dionne — 1 copy

Sandia National Laboratories
ORG. 1231, P.O. Box 5800
Albuquerque, New Mexico 87185
Attn: Dr. Thomas P. Wright — 1 copy
Mr. J.E. Powell — 1 copy
Dr. J. Hoffman — 1 copy
Dr. W.P. Ballard — 1 copy
Dr. C. Clark — 1 copy

Science Applications, Inc.
1710 Goodridge Dr.
McLean, Virginia 22102
Attn: Adam Drobot — 1 copy
P. Vitrello — 1 copy
D. Bacon — 1 copy
C. Menyuk — 1 copy

Stanford University
High Energy Physics Laboratory
Stanford, California 94305
Attn: Dr. T.I. Smith — 1 copy

TRW, Inc.
Space and Technology Group
Suite 2600
1000 Wilson Boulevard
Arlington, VA 22209
Attn: Dr. Neil C. Schoen — 1 copy

TRW, Inc.
Redondo Beach, California 90278
Attn: Dr. H. Boehmer — 1 copy
Dr. T. Romisser — 1 copy

University of California
Physics Department
Irvine, California 92717
Attn: Dr. G. Benford — 1 copy
Dr. N. Rostoker — 1 copy

University of California
Department of Physics
Los Angeles, CA 90024
Attn: Dr. A.T. Lin — 1 copy
Dr. N. Luhmann — 1 copy
Dr. D. McDermott — 1 copy

University of Maryland
Department of Electrical Engineering
College Park, Maryland 20742
Attn: Dr. V. L. Granatstein — 1 copy
Dr. W. W. Destler — 1 copy

University of Maryland
Laboratory for Plasma and Fusion
Energy Studies
College Park, Maryland 20742
Attn: Dr. Jhan Varyan Hellman — 1 copy
Dr. John Finn — 1 copy
Dr. Baruch Levush — 1 copy
Dr. Tom Antonsen — 1 copy
Dr. Edward Ott — 1 copy

University of Tennessee
Dept. of Electrical Engr.
Knoxville, Tennessee 37916
Attn: Dr. I. Alexeff — 1 copy

University of New Mexico
Department of Physics and Astronomy
800 Yale Blvd, N.E.
Albuquerque, New Mexico 87131
Attn: Dr. Gerald T. Moore — 1 copy

University of Utah
Deparment of Electrical Engineering
3053 Merrill Engineering Bldg.
Salt Lake City, Utah 84112
Attn: Dr. Larry Barnett 1 copy
Dr. J. Mark Baird 1 copy

U. S. Naval Academy
Annapolis, Maryland 21402-5021 1 copy

U. S. Army
Harry Diamond Labs
2800 Powder Mill Road
Adelphi, Maryland 20783-1145
Attn: Dr. Edward Brown 1 copy
Dr. Michael Chaffey 1 copy
Dr. Howard Brandt 1 copy

Varian Associates
611 Hansen Way
Palo Alto, California 94303
Attn: Dr. H. Jory 1 copy
Dr. David Stone 1 copy
Dr. Kevin Felch 1 copy
Dr. A. Salop 1 copy

Varian Eimac San Carlos Division
301 Industrial Way
San Carlos, California 94070
Attn: C. Marshall Loring 1 copy

Yale University
Applied Physics
Madison Lab
P.O. Box 2159
Yale Station
New Haven, Connecticut 06520
Attn: Dr. N. Ebrahim 1 copy
Dr. I. Bernstein 1 copy

NRL Records 1 copy

END

DATE

FILMED

DTIC

11-88